Geophys. J. R. astr. Soc. (1987) **91**, 383–411

Computation of high-frequency seismic wavefields in 3-D laterally inhomogeneous anisotropic media

D. Gajewski *Geophysical Institute, Karlsruhe University, Hertzstr. 16, 7500 Karlsruhe-West, F.R.G.*

I. Pšenčík *Geophysical Institute, Czechosl.Acad.Sci., Boční II, 141 31 Praha 4, Czechoslovakia*

Accepted 1987 June 29. Received 1987 June 29; in original form 1987 March 3

Summary. An algorithm for the computation of travel times, ray amplitudes and ray synthetic seismograms in 3-D laterally inhomogeneous media composed of isotropic and anisotropic layers is described. All 21 independent elastic parameters may vary within the anisotropic layers. Rays and travel times are evaluated by numerical solution of the ray tracing equations. Ray amplitudes are determined by evaluating reflection/ transmission coefficients and the geometrical spreading along individual rays. The geometrical spreading is computed approximately by numerical measurement of the cross-sectional area of the ray tube formed by three neighbouring rays. A similar approximate procedure is used for the determination of the coefficients of the paraxial ray approximation. The ray paraxial approximation makes computation of synthetic seismograms on the surface of the model very efficient. Examples of ray synthetic seismograms computed with a program package based on the described algorithm are presented.

1 Introduction

For years, the interest in the propagation of seismic waves in anisotropic media was mostly theoretical. At present, however, the importance of the practical aspects is considerably increasing. A large quantity of data which indicates the presence of anisotropy in the Earth's crust and the upper mantle has been collected in many regions of the world. The anisotropy of a medium is often closely connected with complex inhomogeneity of the medium. Thus methods which allow the study of seismic wave propagation in complex laterally varying layered structures, containing combinations of isotropic and anisotropic layers, are highly desirable.

Various high-frequency asymptotic methods have a good record in investigations of laterally inhomogeneous isotropic structures. It is therefore natural to apply the most widespread of them - the ray method - to the problems of the propagation of seismic waves in inhomogeneous anisotropic media.

The ray method is a high-frequency asymptotic technique, which can only be applied if the wave and medium parameters vary slowly within a wavelength. The results obtained with the ray method are of limited accuracy in singular regions, such as in the vicinity of a caustic, cusp point or critical point, a transition from the illuminated to the shadow region, or a region where the velocities of two quasi-shear waves are locally almost identical. The results obtained with the ray method are also sensitive to some extent to the way in which the approximation of the model parameters is done. On the other hand, the ray method can be applied to more complex models where other methods fail. The computations based on the ray method are usually the fastest when compared with other methods. A very valuable property of the ray method is its ability to single out individual parts of the total wave field and investigate them independently. This gives a clear insight into the formation of the total wave field.

If the limitations of the method are kept in mind, the ray method can very effectively give important results concerning the propagation of seismic waves in inhomogeneous isotropic and anisotropic media.

The ray theory of the propagation of seismic waves in laterally inhomogeneous anisotropic media has been known for a long time. The papers by Babich (1961) and Červený (1972) represent the pioneering work in this field. For a long time the theory in these papers was only applied to specific simplified problems, mostly to the computation of travel times. It was also used in an approach based on linearization for the computation of travel times in weakly anisotropic media (Červený and Firbas 1984). An algorithm for the computation of travel times and vectorial ray amplitudes in 3D inhomogeneous anisotropic media has been suggested and described only recently by Petrashen and Kashtan (1984).

In this paper we describe an algorithm based mostly on the formulae derived by Babich (1961) and Červený (1972). The programs based on the algorithm may be used to compute travel times, ray amplitudes and ray synthetic seismograms of seismic body waves propagating in 3D laterally inhomogeneous models composed of perfectly elastic isotropic and anisotropic layers. All 21 elastic parameters may vary within the anisotropic layers. No assumption of weak anisotropy, and therefore, no linearization is used. A similar algorithm and programs for models composed of isotropic and transversely isotropic inhomogeneous layers were developed recently by Hanyga (1986a).

Since the theory of the propagation of high-frequency seismic waves in inhomogeneous isotropic and anisotropic media has been described in sufficient detail in many papers and textbooks (Babich 1961, Červený 1972, Červený *et al.* 1977, Červený & Firbas 1984, Crampin 1981, Petrashen and Kashtan 1984, Červený 1985, Hanyga 1986b), only the final, most important formulae are presented without derivation.

The basic formulae of the ray theory of propagation of seismic waves in inhomogeneous, anisotropic media can be found in Section 2. The most important steps in the algorithm for the computation of ray synthetic seismograms are described in Section 3, which contains a description of the possible types of model, the computation of rays and amplitudes, the approximate methods of evaluation of geometrical spreading, and the paraxial ray approximation. Simple examples of results obtained with program packages based on the described algorithm for a model of anisotropic subcrustal lithosphere are presented in Section 4 (results of more extensive computations for the same model of the lithosphere can be found in Gajewski and Pšenčík 1987). In Section 5, the possibilities of the algorithm, and the programs based on it, are summarized and possible further generalizations are briefly discussed.

The component notation for vectors and matrices is used throughout the paper, the components often being referred to as vectors or matrices. The indices have always the form of righthand suffices. The lower-case indices take values 1, 2 and 3, the capital-letter indices take values 1 and 2. The Einstein summation convention applies over repeated indices. Partial derivatives with respect to the Cartesian coordinates x_j and time t may be denoted as follows: $u_{i,j} = \partial u_i/\partial x_j$, $u_{i,t} = \partial u_i/\partial t$.

2 Ray method for anisotropic laterally varying layered media

2.1 BASIC EQUATIONS

The equation of motion in an inhomogeneous, perfectly elastic anisotropic medium has the following form

$$(c_{ijkl}u_{k,l})_{,i} = \rho u_{j,tt}, \tag{2.1}$$

where u_i is a displacement vector, $c_{ijkl} = c_{ijkl}(x_m)$ is a fourth order tensor of elastic parameters, $\rho = \rho(x_m)$ is the density, m=1,2,3 and t is time.

We seek an approximate solution of Eq. (2.1) in the form common to high-frequency asymptotic methods (zero order ray approximation):

$$u_i(x_j,t) = U_i(x_j)\exp\left(-i\omega[t-\tau(x_j)]\right). \quad (2.2)$$

The amplitude vector $U_i(x_j)$, which may be generally complex-valued, and the phase function (eikonal) $\tau(x_j)$ are the quantities to be determined. ω is the circular frequency. To determine U_i and τ, (2.2) is inserted into (2.1). This yields the basic system of equations of the ray method for inhomogeneous anisotropic media,

$$(\Gamma_{jk}-\delta_{jk})U_k = 0, \quad (2.3)$$

$$a_{ijkl}p_iU_{k,l} + \rho^{-1}(\rho a_{ijkl}p_lU_k)_{,i} = 0. \quad (2.4)$$

The following notation is used in (2.3) and (2.4):

$$\Gamma_{jk} = a_{ijkl}p_ip_l, \; p_i=\tau_{,i} \;, \; a_{ijkl}=c_{ijkl}/\rho \quad (2.5)$$

The partial derivatives of the phase function with respect to x_i are the components of the slowness vector p_i, the vector perpendicular to the wavefront $\tau(x_j) = t$, and thus parallel to the wave normal vector. The matrix Γ_{jk} is positive definite.

It is obvious that a necessary condition for the solution of (2.3) is

$$\det(\Gamma_{jk}-\delta_{jk}) = 0. \quad (2.6)$$

The condition (2.6) is satisfied if at least one of the eigenvalues $G(x_j,p_j)$ of the matrix Γ_{jk}, is equal to one;

$$G(x_j,p_j) = a_{ijkl}p_ip_lg_jg_k = 1. \quad (2.7)$$

The eigenvector $g_i(x_j,p_j)$ corresponding to the eigenvalue (2.7) determines the orientation of the corresponding amplitude vector U_i,

$$U_i(x_j) = A(x_j)g_i(x_j,p_j). \quad (2.8)$$

The eigenvector g_i may also be called a polarization vector, and is defined as a unit vector. If the slowness vector corresponding to g_i is complex (this occurs in the case of over-critical incidence of a wave at an interface), the polarization vector also becomes complex. $A(x_j)$ is a scalar amplitude.

If the matrix Γ_{jk} has three different eigenvalues, then three independent waves exist: one quasi-*P* (*qP*) wave, and two quasi-shear waves, (*qS*1 and *qS*2). At a point in a medium, for one wave normal direction (specified by the slowness vector p_i), these three waves have mutually perpendicular polarization vectors. This is a very special situation, however, as generally the three waves propagate independently along different paths with different wave normal directions. Thus at points where all three waves can be observed, the polarization vectors are usually not perpendicular.

Generally, the polarization vector of a *qP*-wave is not perpendicular to the wavefront, and the polarization vectors of *qS*-waves are not situated in the tangential plane to the wavefront. The *qP*-wave is always faster than the *qS*-waves, independent of the orientation of its polarization vector. The definition of the *qP*-wave as the fastest wave is preferable to the definition of the *qP*-wave as the wave with the polarization vector closest to the wave normal (Fedorov 1968). Dellinger and Muir (1986) showed that even in highly symmetric anisotropic media the polarization vector of a *qP*-wave could be, in principle, perpendicular to the wave normal.

The fact that the two *qS*-waves propagate independently is referred to as shear-wave splitting or shear-wave double refraction.

If the matrix Γ_{jk} has two coinciding eigenvalues, the two *qS*-waves propagate with the same phase velocity (not more than two eigenvalues may coincide, and they are always the eigenvalues corresponding to *qS*-waves, see Musgrave (1970), p102). Such a situation may occur locally when the slowness vector coincides with a symmetry axis (Fedorov 1968). In an isotropic medium it occurs everywhere. The isotropic medium represents a degenerate case of an anisotropic medium, in which any direction represents a symmetry axis. In the isotropic medium, the polarization vector of a *qP*-wave is parallel to the corresponding slowness vector, and is thus perpendicular to the wavefront. The polarization vectors of the shear waves are perpendicular to the corresponding slowness vector, and thus situated in the plane tangential to the wavefront. The orientation of the polarization vectors of *qS*-waves in this plane is non-uniquely determined (so called degenerate polarization, see Kravtsov & Orlov 1980). Thus, in this case any two mutually orthogonal unit vectors situated in the plane tangential to the wavefront may be chosen as polarization vectors of *qS*-waves.

2.2 COMPUTATION OF RAYS, PHASE FUNCTIONS AND AMPLITUDES

Solving the eikonal equation (2.7) leads to the ray tracing system for anisotropic media (Červený & Firbas 1984):

$$dx_i/d\tau = a_{ijkl}\, p_l g_j g_k, \quad dp_i/d\tau = -1/2(a_{mjkl})_{,i}\, p_m p_l g_j g_k. \tag{2.9}$$

The phase function τ, which plays a role of a parameter along a ray in (2.9), gives the travel time along the ray. The elastic parameters a_{ijkl} are assumed to be known at all points in the medium. The eigenvectors g_i can be determined in the way described in Section 3.3.2. Equations (2.9) yield the values of phase velocity V, $V = (p_j p_j)^{-1/2}$, and of the group velocity v, $v = (v_j v_j)^{1/2}$, where v_j are the components of the group velocity vector, $v_j = dx_j/d\tau$ (the group velocity vector specifies the direction of the energy flux).

The ray tracing system (2.9) can be rewritten in a different form if explicit expressions for $g_j g_k$ suggested by Červený (1972), Červený et al. (1977) are used:

$$g_j g_k = D_{jk}/D, \tag{2.10}$$

where

$$\left.\begin{aligned} D_{11} &= (\Gamma_{22}-1)(\Gamma_{33}-1) - \Gamma_{23}^2, \quad D_{12} = D_{21} = \Gamma_{13}\Gamma_{23} - \Gamma_{12}(\Gamma_{33}-1),\\ D_{22} &= (\Gamma_{33}-1)(\Gamma_{11}-1) - \Gamma_{13}^2, \quad D_{13} = D_{31} = \Gamma_{12}\Gamma_{23} - \Gamma_{13}(\Gamma_{22}-1),\\ D_{33} &= (\Gamma_{11}-1)(\Gamma_{22}-1) - \Gamma_{12}^2, \quad D_{23} = D_{32} = \Gamma_{12}\Gamma_{13} - \Gamma_{23}(\Gamma_{11}-1),\\ D &= D_{11} + D_{22} + D_{33}. \end{aligned}\right\} \tag{2.11}$$

A disadvantage of this formulation is that (2.11) cannot be used in situations in which Γ_{jk} has two identical eigenvalues, for example in isotropic media, since then $D = 0$. In isotropic media the ray tracing system (2.9) with the right hand sides expressed using (2.10) and (2.11) is substituted by the following ray tracing system (Červený et al. 1977):

$$dx_i/d\tau = v^2 p_i, \quad dp_i/d\tau = -v^{-1} v_{,i}, \tag{2.12}$$

with $v = V$.

The ray tracing system (2.9) or (2.12) can be solved numerically if the appropriate initial conditions are specified. They can be specified as follows:

$$x_i(\tau_0) = x_{0i}, \quad p_i(\tau_0) = p_{0i}, \tag{2.13}$$

where x_{0i} are the coordinates of the initial point of the ray (the source) and p_{0i} are the components of the slowness vector at the same point. The quantities p_{0i} must satisfy (2.7).

The second basic equation of the ray method, (2.4) can be transformed into a transport equation and solved with the use of the ray coordinates. The ray coordinates γ_1, γ_2, τ can be introduced as follows. The coordinates γ_1, γ_2 are the ray parameters specifying a ray. They may be chosen *e.g.* as take-off angles at the source. The third ray coordinate is the travel time along the ray. In an isotropic medium, the coordinate line specified by fixed γ_1, γ_2 (the ray) is perpendicular to the coordinate surface specified by fixed τ (the wavefront). In an anisotropic medium this is generally not the case.

The solution of the transport equation may be written as follows,

$$A(\tau) = \Psi(\gamma_1,\gamma_2)\ [\rho(\tau)V(\tau)J(\tau)]^{-1/2}. \tag{2.14}$$

This relation holds in both anisotropic and isotropic media. It determines the scalar amplitude along a ray specified by the ray parameters γ_1, γ_2. The space dependence of the functions A, V, ρ and J is expressed in (2.14) through the space dependence of the phase function $\tau = \tau(x_j)$ along the ray.

The product of the phase velocity V and the function J in (2.14) is the Jacobian of the transformation from ray coordinates γ_1, γ_2, $\gamma_3 = \tau$ to Cartesian coordinates x_i,

$$VJ = \det\ (\partial x_i/\partial g_j). \tag{2.15}$$

Function J itself is a measure of the size of the cross-section of the ray tube with the wavefront.

Function Ψ is constant along a ray, but its value generally differs for different rays. Using this property of Ψ, we can rewrite (2.14) in another useful form,

$$A(\tau) = \Big([\rho(\tau_0)V(\tau_0)]/[\rho(\tau)V(\tau)]\Big)^{1/2} L^{-1}(\tau), \tag{2.16}$$

where the quantity $L(\tau)$,

$$L(\tau) = [J(\tau)/J(\tau_0)]^{1/2} \tag{2.16$'$}$$

is the geometrical spreading. If $L = 1$ is inserted into (2.16), Equation (2.16) gives the expression for the scalar spreading-free amplitude.

2.3 INFLUENCE OF INTERFACES

Additional formulae must be supplied to those presented in the preceding section if the considered models contain interfaces of the first order, i.e. interfaces at which at least one of the elastic parameters or the density changes discontinuously. These additional formulae describe the transformation of the computed quantities across interfaces. The quantities to be transformed are the slowness vector and scalar amplitudes.

A body wave incident on an interface of the first order in an anisotropic medium may generate three reflected and three transmitted waves, in an isotropic medium only two waves of each kind. As for isotropic media, in the high-frequency approximation the problem of reflection/transmission of an arbitrary body wave at a curved interface separating anisotropic media reduces to the problem of reflection/ transmission of a plane wave at a plane interface. The latter problem is well covered in the literature (Fedorov 1968, Musgrave 1970, Henneke 1972, Šílený 1981), and therefore it will be only briefly described.

The selection of the type of the generated wave is controlled by the numerical code.

2.3.1 *Transformation of the slowness vector across an interface*

The slowness vector of a generated wave is sought in the form (Fedorov 1968);

$$p_i = b_i + \xi n_i . \qquad (2.17)$$

In (2.17), n_i is the unit normal vector to the interface, pointing into the medium in which the incident wave propagates. The vector b_i is the vectorial component of the slowness vector in the plane tangential to the interface. The vector b_i is the same for all generated waves, as well as the incident wave. The quantity ξ, representing the projection of the slowness vector on the normal to the interface n_i, is to be determined. Inserting (2.17) into (2.6) with the elastic parameters from the medium in which the generated waves propagate, yields a sixth order polynomial equation in ξ. Some of its roots may be complex, and these correspond to generated inhomogeneous waves. The roots belonging to the homogeneous waves are real. The selection of the root corresponding to each generated wave is described in Section 3.3.3.

The above procedure is used if the generated wave propagates in an anisotropic medium. If the generated wave propagates in an isotropic medium, simple explicit expressions for the slowness vector of the generated wave may be used (Červený et al. 1977),

$$\tilde{p}_i = p_i - n_i(C \pm E), \tag{2.18}$$

where

$$C = p_j n_j, \quad E = (\tilde{v}^{-2} - V^{-2} + C^2)^{1/2}. \tag{2.19}$$

In (2.18) and (2.19), a tilde denotes the quantities on the side of the interface where the generated wave propagates. In the considered case, the group velocity $\tilde{v}$ is equal to the phase velocity $\tilde{V}$. The upper sign in (2.18) corresponds to the transmitted wave, the lower one to the reflected wave. The square root for E in (2.19) is taken positive.

2.3.2 Transformation of scalar amplitudes across an interface

The scalar amplitude $\tilde{A}$ of a generated wave at the point of incidence is given by the relation,

$$\tilde{A} = RA, \tag{2.20}$$

where A is the scalar amplitude of the incident wave at the same point. The quantity R in (2.20) denotes a plane wave reflection/transmission coefficient. The coefficient is obtained by solving a system of six linear algebraic equations resulting from the conditions of continuity of displacement and stress across the interface (Fedorov 1968):

$$\left.\begin{aligned} R^{T1}g_i^{T1} + R^{T2}g_i^{T2} + R^{T3}g_i^{R3} - R^{R1}g_i^{R1} - R^{R2}g_i^{R2} - R^{R3}g_i^{R3} &= g_i^{I} \\ R^{T1}\sigma_i^{T1} + R^{T2}\sigma_i^{T2} + R^{T3}\sigma_i^{T3} - R^{R1}\sigma_i^{R1} - R^{R2}\sigma_i^{R2} - R^{R3}\sigma_i^{R3} &= \sigma_i^{I} \end{aligned}\right\} \tag{2.21}$$

for $i = 1, 2, 3$. Here g_i are the Cartesian components of a polarization vector, and σ_i^I on the R.H.S., and $R\sigma_i^{T(R)}$ on the L.H.S. of (2.21) are the Cartesian components of the vector projection of the stress tensor corresponding to the incident wave, and a generated wave respectively, on the normal n_i to the interface,

$$\sigma_i^I = \rho a_{ijkl} n_j p_k A g_l, \quad \sigma_i^{T(R)} = \tilde{\rho}\tilde{a}_{ijkl} n_j \tilde{p}_k A \tilde{g}_l. \tag{2.22}$$

Indices $T1$, $T2$, $T3$ denote the quantities corresponding to the two transmitted qS-waves and one transmitted qP-wave, $R1$, $R2$, $R3$ to the two reflected qS-waves and one reflected qP-wave. Index I corresponds to the incident wave which may be any one of the three types of wave.

In the case of reflection from the free surface, the system reduces to three linear algebraic equations for three reflection coefficients R^{F1}, R^{F2}, R^{F3} from the free surface;

$$R^{F1}\sigma_i^{R1} + R^{F2}\sigma_i^{R2} + R^{F3}\sigma_i^{R3} = -\sigma_i^{I} \tag{2.23}$$

for i = 1, 2, 3.

The solution of system (2.21) or (2.23) requires knowledge of the parameters of the medium and the parameters of the incident wave, as well as knowledge of the eigenvectors of the generated waves at the point of reflection/transmission, and these may be determined as described in Section 3.3.2. If any eigenvector is complex-valued, the reflection/transmission coefficients will also be complex-valued. System (2.21) or (2.23) may be used universally for any combination of anisotropic and isotropic media separated by an interface.

For isotropic media the reflection/transmission coeffients are available in an explicit form (Červený *et al.* 1977, Aki & Richards 1980). If the explicit expressions are used in 3-D isotropic media, one must perform a rotation of the ray-centred coordinate system and its base vectors (polarization vectors) into the local interface coordinate system (in which the coefficients are specified). This transformation must be done once or possibly twice at each point of incidence (Červený 1985). This problem does not arise if the coefficients of reflection/transmission are evaluated by solving (2.21) or (2.23) at each interface, which simplifies the procedure of the evaluation of amplitudes.

Note that the explicit expressions for reflection/transmission coefficients are available even for some types of anisotropic media. For example, Daley and Hron (1977) presented reflection/transmission coefficients for transversely isotropic media.

If the receivers are situated on the surface of the model (which is the case in the algorithm which is used), the free surface conversion coefficients must be evaluated to take into account the waves reflected from the free surface. The conversion coefficients are the components of the conversion vector q_i in the appropriate coordinate system. The conversion vector corresponding to an incident wave *I* has the form,

$$q_i = g_i^{I} + R^{F1}g_i^{R1} + R^{F2}g_i^{R2} + R^{F3}g_i^{R3}. \tag{2.24}$$

In (2.24), R^{F1}, R^{F2}, R^{F3} are again coefficients of the reflection from the free surface corresponding respectively to the two generated *qS*-waves and one *qP*-wave in an anisotropic subsurface layer. In the case of an isotropic subsurface layer, the polarization vectors g_i^{R1}, g_i^{R2} may be chosen in such a way that the reflection coefficients R^{F1} and R^{F2} correspond to the transformation of the incident wave into reflected SV- and SH-waves.

2.4 PARAXIAL RAY APPROXIMATION

The formulae presented in the preceding sections allow the evaluation of the wave field of an elementary wave only at points on a ray. To construct ray synthetic seismograms at a system of receivers distributed on the surface of a model, it is necessary to solve the two-point ray tracing problem, i.e. to construct rays connecting the source with individual receivers. The two-point ray tracing is a complicated and time-consuming procedure, especially in 3-D problems. In 2-D problems, it consists of a search for one ray parameter specifying the required ray, while in 3-D problems it is necessary to search for two independent ray parameters. The number of the ray parameters sought may be reduced to one even in 3-D problems, if instead of the ray connecting the source with a receiver, a ray connecting the source with an arbitrary point of a profile on the surface of the model is sought. This is called boundary-value ray tracing. If initial-value ray tracing is performed, where the rays are specified only by the position of the source and their direction at the source, with the position of the endpoints being *a priori* unknown, no search for the ray parameters is required. For the evaluation of the wavefield at specified receivers in the last two cases mentioned, it is necessary to use a procedure which makes possible the evaluation of the wavefield in the vicinity of computed rays. This procedure is the paraxial ray approximation (Červený *et al.* 1984, Červený 1985).

The formulae for the paraxial ray approximation may be obtained by expanding (2.2) in the vicinity of a ray Ω. For the phase function τ at a point x_i situated in the vicinity of a point $\bar{x}_i$ on the ray Ω, the Taylor expansion of the phase function τ gives

$$\tau(x_j) = \tau(\bar{x}_j) + p_k(\bar{x}_j).(x_k-\bar{x}_k) + \frac{1}{2} N_{ik}(\bar{x}_j).(x_i-\bar{x}_i).(x_k-\bar{x}_k) \qquad (2.25)$$

In (2.25), $p_k(\bar{x}_j) = \partial\tau/\partial x_k|_{\bar{x}_j}$ are the components of the slowness vector, $N_{ik}(\bar{x}_j) = \partial^2\tau/\partial x_k \partial x_i|_{\bar{x}_j}$ are the elements of a matrix of the second partial derivatives of the travel time field with respect to the Cartesian coordinates.

For the determination of the amplitude vector in the vicinity of the ray Ω, equation (2.8) is used in the same form as before. The polarization vector $g_i(x_j,p_j)$, however, is to be determined from (2.3) with U_k

substituted by g_k, where Γ_{jk} is specified as follows,

$$\Gamma_{jk}(x_m) = p_i(x_m) \cdot p_l(x_m) \cdot a_{ijkl}(x_m), \tag{2.26a}$$

$$p_n(x_m) = p_n(\bar{x}_m) + N_{kn}(\bar{x}_m) \cdot (x_k - \bar{x}_k). \tag{2.26b}$$

In an isotropic medium, the approximate expressions for the polarization vectors may be obtained in an explicit form.

For *P*-waves:

$$g_i(x_j, p_j) = v(\bar{x}_j) \cdot p_i(\bar{x}_j) + v(\bar{x}_j) \cdot N_{ik}(\bar{x}_j) \cdot (x_k - \bar{x}_k), \tag{2.27a}$$

which immediately follows from (2.26b). For *S*-waves,

$$g_{Ii}(x_j, p_j) = e_{Ii}(\bar{x}_j) - N_{kl}(\bar{x}_j) \cdot v(\bar{x}_j) \cdot p_i(\bar{x}_j) \cdot e_{Ik}(\bar{x}_j) \cdot (x_l - \bar{x}_l), \tag{2.27b}$$

In (2.27), e_{Ik} are the components of the *I*-th unit vector of the vectorial base of the ray-centred coordinate system, situated in the plane perpendicular to the slowness vector at x_j, or, in other words, in the plane tangent to the wavefront at x_j (Červený et al. 1984, Červený 1985).

2.5 COMPUTATION OF RAY SYNTHETIC SEISMOGRAMS

Up to now we have only considered a single elementary wave and shown how the characteristics of this wave may be computed. From the phase function $\tau(x_j)$ and complex-valued vectorial amplitude $U_k(x_j)$, an elementary seismogram may be constructed for the given source-time function in several ways (Červený et al. 1977, Červený 1985). Summing up all elementary seismograms corresponding to elementary waves arriving at a receiver, we obtain the ray synthetic seismogram at the receiver.

3 Algorithm

The algorithm of the computation of travel times, vectorial amplitudes, and ray synthetic seismograms for 3-D laterally inhomogeneous media composed of isotropic and anisotropic layers with the use of the formulae presented in the preceding sections, consists of the following main steps: (1) Specification of the model; (2) Specification of the source; (3) Ray tracing including the determination of the phase function along the computed rays from the source to the region where the receivers are situated; (4) The evaluation of complex-valued vectorial spreading-free amplitudes along the rays; (5) The evaluation of the geometrical spreading for each ray and the paraxial ray approximation to determine the travel times and complex-valued vectorial amplitudes at specified receivers; (6) The construction of the ray synthetic seismograms.

In the following sections each of these steps is described in some detail.

3.1 SPECIFICATION OF THE MODEL

A 3-D model of a laterally inhomogeneous structure composed of isotropic and anisotropic layers separated by curved non-intersecting interfaces is considered. The model is situated in a "box" specified in Cartesian coordinates by the relations

$$x_m^{min} \leq x_m \leq x_m^{max}, \quad m = 1, 2, 3. \tag{3.1}$$

The coordinate axes x_1, x_2 are situated in the horizontal plane, the x_3-axis is vertical. The anisotropic layers are described by the distribution of, in general, 21 elastic parameters $c_{ijkl}(x_m)$ and density $\rho(x_m)$. Instead of the parameters c_{ijkl}, the parameters a_{ijkl}, defined in (2.5), are used, and also called elastic parameters. The isotropic layers are described by the distribution of P- and S-wave velocities, $v_P(x_m)$, $v_S(x_m)$, and density $\rho(x_m)$. Inside the layers, the parameters a_{ijkl}, velocities v_P, v_S and density ρ vary continuously with their first and second partial derivatives. The layers are separated by curved interfaces at which a_{ijkl}, v_P, v_S, ρ, or their first or second derivatives may change discontinuously.

The interfaces are smooth surfaces

$$x_3 = f(x_1,x_2), \tag{3.2}$$

defined on the whole intersection of the model "box" with a horizontal plane. The functions $f(x_1,x_2)$ are continuous together with their first and second partial derivatives in the whole region of definition. The interfaces may neither intersect each other nor the horizontal boundaries of the model ($x_3 = x_3^{min}$ and $x_3 = x_3^{max}$). Each interface is specified on an independent horizontal rectangular grid. Bicubic splines (possibly with smoothing) are used to approximate the interfaces.

The elastic parameters a_{ijkl} may be specified in a coordinate system whose axes coincide with the principal axes of the elasticity tensor. Such a system is very practical since in it many of the elastic parameters are zero. Thus, the amount of input data can be considerably reduced. Together with the elastic parameters, the angles specifying the orientation of the principal axes with respect to the general Cartesian coordinate system must be specified.

The variation of elastic parameters or velocities of P- and S-waves, and the density inside the layers may be specified in two ways: 1. Variation with depth only; 2. Linear variation along vertical lines between interfaces representing isosurfaces of elastic parameters.

In the first case, the parameters are specified at several depths in each layer and then approximated by cubic splines. In this way the distribution of elastic parameters is laterally homogeneous, only the thickness of the layers may vary due to the curved or inclined interfaces.

In the second case, the elastic parameters are specified as constant along interfaces, the interfaces thus being isosurfaces of the parameters. Linear interpolation of the parameters along vertical lines is used between interfaces bounding a layer. In this way, the distribution of the parameters in the layers with curved interfaces is laterally inhomogenous. Vertical gradients are larger in regions where the layers are thinner, and smaller, where the thickness of the layers is larger. A broad variety of models may be simulated by this approximation. This approximation requires a considerably reduced amount of data storage in comparison with other 3-D approximations (*e.g.* approximations on 3-D grids). For each layer, only two sets of parameters are required while in grid approximations one set must be specified for each grid point. There is a disadvantage with this approach in that the isosurfaces represent interfaces of the second order, the existence of which influences the behaviour of ray amplitudes. However, that may be controlled and corrected. The fact that the interfaces represent isosurfaces of elastic parameters limits the range of application of this approximation with respect to models of realistic structures. It is, however, not difficult to remove this problem for future applications.

The density at any point of the model is determined from the relation

$$\rho = a + bv_P, \tag{3.3}$$

where a and b are constants generally different for each layer, v_P is the P-wave velocity in an isotropic layer or square root of the elastic parameter a_{1111} in an anisotropic layer.

3.2 SPECIFICATION OF THE SOURCE

A point source, which may be situated at any point of the model is considered. The computation of rays and travel times from such a source is performed as described in Section 3.3.1. The computation of amplitudes from the point source situated in an anisotropic medium can be performed in the way described e.g. by Hanyga (1984). Here, for simplicity, we present only formulae for a point source situated in an isotropic medium. The function Ψ from (2.14) has in this case the following form:

$$\Psi(\phi_0, \delta_0) = \left[\rho(\tau_0) v(\tau_0) \cos\delta_0\right]^{1/2} g(\phi_0, \delta_0). \tag{3.4}$$

The ray parameters ϕ_0, δ_0 are the take-off angles ($0 \leq \phi_0 \leq 2\pi$, $-\pi/2 \leq \delta_0 \leq \pi/2$) specifying the initial direction of the wave normal N_i at the source,

$$N_1 = \cos\phi_0 \cos\delta_0, \; N_2 = \sin\phi_0 \cos\delta_0, \; N_3 = \sin\delta_0. \tag{3.5}$$

In isotropic media, the take-off angles also specify the initial direction of the ray at the source. In anisotropic media, however, the initial direction of the ray differs from that specified by the take-off angles.

The quantities $\rho(\tau_0)$, $v(\tau_0)=V(\tau_0)$ in (3.4) are the density and velocity of the corresponding wave at the source. The function $g(\phi_0, \delta_0)$ specifies the frequency-independent radiation pattern. Radiation patterns of various sources of seismological importance may be used, and appropriate expressions can be found, for example, in Aki & Richards (1980). As a source-time function, we use the Gaussian envelope signal

$$f(t) = \exp[(2\pi f_M/\gamma)^2] \cos(2\pi f_M t + \nu), \tag{3.6}$$

where f_M, γ and ν are the parameters of the signal. f_M is its dominant frequency.

For testing purposes, an artificial point source, situated in an isotropic layer and radiating both *P*- and *S*-waves is used. The radiation pattern $g(\phi_0, \delta_0)$ is constant and different for *P*- and *S*-waves. The orientation of the polarization vector of *P*-waves at the source is specified to be parallel to the slowness vector. The polarization vector of *S*-waves at the source may be chosen arbitrarily in the plane perpendicular to the slowness vector.

3.3 COMPUTATION OF RAYS AND TRAVEL TIMES

3.3.1 *Start of the computation of rays*

To start the computation of rays, the initial conditions (2.13) must be specified. For this purpose, the components of the slowness vector may be expressed through the components of the wave normal N_i,

$$p_i = N_i/V \tag{3.7}$$

Here, V is the phase velocity of the considered wave. In isotropic media, V depends only on the position in the medium, and equals the group velocity v. It may be immediately determined from the distribution of P- and S-wave velocities in the model. In anisotropic media, V depends not only on the position in the medium but also on the orientation of the wave normal. It may be determined from the equation

$$\det(a_{ijkl}N_iN_l-V^2\delta_{jk}) = 0, \tag{3.8}$$

which follows from (2.6), where (3.7) was used for p_i. The wave normal at the source is determined from (3.5). Equation (3.8) is a cubic equation for the squares of the phase velocity. Since Γ_{jk} is positive definite, its roots are always real and positive. To solve (3.8), Cardano's method of solving cubic equations is used. From the three determined velocities, the proper one is selected according to the numerical code, which specifies the type of the wave on its way from the source. The selection of qP-wave phase velocity is straightforward. There is, however, a certain problem with the selection of the proper qS phase velocity. If necessary, the two qS phase velocities may be distinguished by the orientation of the corresponding polarization vectors (their determination is described below). But generally both qS-waves are equally important in forming final synthetics, and should be considered together. This means in principle, that the waves propagating in anisotropic media can be described by numerical codes designed for isotropic media (which distinguish only two types of waves).

3.3.2 *Determination of polarization vectors*

In an anisotropic layer, the polarization vectors may be determined from the quantities D_{ij}. For a given slowness vector the matrix D_{ij} can be computed from (2.5) and (2.11). Each line or column of the matrix D_{ij} is proportional to the eigenvector, thus to obtain g_i, one line of D_{ij} must be normalized to form a unit vector. The above procedure may always be used for qP-waves, but for qS-waves it fails if the matrix Γ_{jk} has two identical eigenvalues (D=0). In the latter case, we may use the same procedure as the following one for isotropic layers.

In isotropic layers the determination of the polarization vector of a P-wave is straightforward. The polarization vectors of shear waves are situated in the plane tangent to the wavefront and any two mutually perpendicular unit vectors in this plane may be chosen as the polarization vectors. The most natural procedure is to choose them identical with the base vectors of the ray centred coordinate system. A detailed description of this coordinate system together with the methods of its determination can be found in Červený (1985), see also Červený et al. (1987). This procedure of the evaluation of the polarization vectors is effective even in the case of local singularities of an anisotropic medium, when the trace of matrix D_{ij} is zero.

3.3.3 *Reflection/transmission*

When the ray intersects an interface, an iterative search for the point of intersection is performed. The accuracy of the determination of the point of intersection can be prescribed.

At the point of intersection, the procedure described in Section 2.3.1 is used to determine the slowness vector of the generated wave. In the case that the ray of the generated wave is situated in an isotropic medium, explicit formulae (2.18) can be used. If the medium is anisotropic, the sixth order polynomial equation in ξ, see (2.17) for ξ, must be solved. Standard procedures for determination of roots of polynomial equations may be used. Not all the roots found are acceptable. First, all complex roots are excluded since they correspond to generated inhomogeneous waves, which are not considered in the algorithm. From the remaining real roots, only those which yield the energy flux vector pointing into the layer in which the generated wave propagates are selected, see Henneke (1972). This is the case if the expression

$$n_i v_i = n_i a_{ijkl} p_l g_j g_k \tag{3.9}$$

is, for given ξ, positive for reflected waves or negative for transmitted waves.

Note that a situation may occur in which the slowness vector points into the layer in which the generated wave is to propagate, but the corresponding energy flux vector points into the other layer, and thus the corresponding root ξ cannot be accepted. On the other hand it may happen that the slowness vector points into the other layer than the one in which the generated wave should propagate, but the corresponding root ξ is accepted since the energy flux vector points into the right layer. Special situations which may occur during an incidence of a wave at an interface between two anisotropic media, such as those described above, are discussed in detail in Henneke (1972) and Šílený (1981).

When the only acceptable roots ξ have been selected, the proper one is chosen in accordance with the numerical code of the investigated wave. The selection of the root corresponding to the qP-wave is simple since the qP-wave is the fastest one. The same argument as that used at the end of Section 3.3.1 may be used for the selection of the proper root of the two qS-waves. The special situations mentioned above must be treated with particular care.

3.3.4 *Ray tracing*

When the take-off angles ϕ_0 and δ_0 are specified, the computation of the ray may begin. In the present algorithm we use the ray tracing system (2.9) with (2.10) and (2.11) to compute rays in anisotropic layers, and (2.12) to compute rays in isotropic layers. Any of the standard procedures for solving systems of ordinary differential equations may be used to solve the ray tracing system. In the present versions of programs based on the described algorithm the Runge-Kutta procedure is used.

Tests have been made which have shown that if the ray paths are mostly in anisotropic layers, it is possible to use ray tracing system (2.9) in all layers, including isotropic layers. In this case, the polarization vectors are evaluated explicitly at each point of the ray instead of using (2.10), (2.11) for the evaluation of the right-hand sides of (2.9).

The rays may be computed from the source to their endpoint, using the method described above. It is desirable that the rays end either at or near receivers. Hovever, many rays may terminate before they reach this region. Some reasons for their early termination may be: the incidence on any of the vertical boundaries of the model, overcritical incidence at an interface, a shear wave singularity (D=0) on the ray path, and others.

The procedure described above is initial-value ray tracing, which yields rays which start from the source in a specified direction (specified by the slowness vector). For the rays starting from the source and terminating at a profile on the surface of the model (boundary-value ray tracing), the above procedure of the initial-value ray tracing is put into an iterative loop. Within the loop, the initial conditions of rays are successively modified so that the rays converge to the ray terminating on the profile. To solve this problem, it is sufficient to vary only one of the two ray parameters. For this purpose, the procedures devised for two-point ray tracing in 2-D models are effective.

3.4 COMPUTATION OF SPREADING-FREE VECTORIAL AMPLITUDES

The computation of spreading-free vectorial amplitudes along a known ray may be performed by means of equations (2.8), (2.14), (2.16), (2.20) and

(2.24), in which the final value of the geometrical spreading L is substituted by a unit.

The spreading-free vectorial amplitudes contain products of the terms of the following type:

$$R(\tilde{\rho}\tilde{V}\cos\tilde{i})^{1/2}/(\rho V\cos i)^{1/2}, \qquad (3.10)$$

where ρ, V represent the density and phase velocity, and i is the acute ray incidence angle subtended with the normal to the interface. The quantities without a tilde correspond to the incident ray at the point of incidence, while the quantities denoted by a tilde have the same meaning but refer to the ray of the generated wave. R in (3.10) denotes the appropriate reflection/transmission coefficient, which can be found by solving the system of six or three linear algebraic equations, see (2.21) or (2.23). Cramer's method is used to solve the system of equations.

The spreading-free vectorial amplitudes also contain the function Ψ, see (3.4), and may contain surface conversion coefficients, see (2.24). The orientation of the spreading-free vectorial amplitudes is specified by the polarization vectors g_i. Their computation is described in Section 3.3.2.

3.5 GEOMETRICAL SPREADING AND PARAXIAL RAY APPROXIMATION

The determination of the geometrical spreading and the matrix of the second derivatives of the travel time field N_{ik} are related problems. One possible method of their determination is the application of dynamic ray tracing along the computed rays: for isotropic media see e.g. Červený (1985), Červený et al. (1987); for anisotropic media, this approach is described in Červený (1972), Hanyga (1986b) and applied by Hanyga (1986a).

In the algorithm which is presented here, a different approach is chosen. Both the geometrical spreading and the matrix N_{ik} are determined approximately from the travel time information on three neighbouring rays. The partial derivatives which appear in the expressions of the geometrical spreading and the matrix N_{ik} are substituted by finite differences. This approach, only applied to the evaluation of the geometrical spreading, has been used quite successfully for isotropic media in earlier versions of package SEIS83, (Červený and Pšenčík 1984), and also by McMechan and Mooney (1980).

The approach is expected to be faster than dynamic ray tracing, and gives sufficiently accurate results if the grouping of endpoints of rays in the investigated region is dense enough. The approach is very efficient if the wave field is evaluated at receivers in groups. Its efficiency decreases if the receivers are isolated, and for the determination of the geometrical spreading and the matrix N_{ik} at each receiver two extra rays must be computed. The approach allows the detection of the effect of a single caustic on the ray path. If a ray touches caustics more than once, the resulting phase shift cannot be properly accounted for.

Let us rewrite the matrix N_{ik} in the following form

$$N_{ik} = \frac{\partial^2\tau}{\partial x_i \partial x_k} = \frac{\partial p_i}{\partial x_k} = \frac{\partial p_i}{\partial \gamma_j}\frac{\partial \gamma_j}{\partial x_k} = Y_{ij}(X^{-1})_{jk} \tag{3.11}$$

The matrix N_{ik} is in (3.11) expressed in terms of two 3 x 3 matrices $X_{ij} = \partial x_i/\partial\gamma_j$ and $Y_{ij} = \partial p_i/\partial\gamma_j$, where γ_j are the ray coordinates, ϕ_0, δ_0 and τ. We can see that the components X_{i3} and Y_{i3} can be obtained immediately from the ray tracing equations since

$$X_{i3} = dx_i/d\tau, \; Y_{i3} = dp_i/d\tau. \tag{3.12}$$

The determination of the remaining elements is more complex. We evaluate them approximately, using two auxiliary rays in the close vicinity of a considered ray, called a *central* ray. The ray coordinates γ_1, γ_2 of the two rays only differ by small quantities $\Delta\gamma_1$, $\Delta\gamma_2$ from the ray coordinates of the central ray. The elements X_{iJ}, Y_{iJ} are the derivatives of x_i and p_i taken at constant $\gamma_3 = \tau$, i.e. along the wavefront. We therefore determine first the points and slowness vectors on the auxiliary rays which approximately correspond to the time τ. For this purpose, we may use ray tracing equations (2.9) which yield the approximations (for small $\tau-\tau^S$):

$$\left.\begin{aligned} x_i(\tau) &= x_i(\tau^S) + a_{ijkl}p_l g_j g_k(\tau - \tau^S), \\ p_i(\tau) &= p_i(\tau^S) - \tfrac{1}{2}(a_{mjkl})_{,i}p_m p_l g_j g_k(\tau - \tau^S), \end{aligned}\right\} \tag{3.13}$$

where τ^S denotes the travel time at the endpoint of an auxiliary ray. The quantities a_{ijkl}, p_i, g_i are all evaluated at this endpoint.

For the point $x_i(\tau)$ on one of the auxiliary rays we use the approximation

$$x_i(\gamma_1 + \Delta\gamma_1, \gamma_2 + \Delta\gamma_2) \simeq x_i(\gamma_1,\gamma_2) + X_{i1}\Delta\gamma_1 + X_{i2}\Delta\gamma_2. \tag{3.14}$$

Similar expressions can be written for the point $x_i(\tau)$ on the other auxiliary ray and for the components of the slowness vectors $p_i(\tau)$ on both auxiliary rays. The resultant equations form two sets of linear algebraic equations for the determination of X_{iJ} and Y_{iJ}. The solution of the system may be written explicitly

$$\left.\begin{aligned} Z_{i1} &= (\Delta z_{i1}\Delta\gamma_{22}-\Delta z_{i2}\Delta\gamma_{21})B^{-1} \\ Z_{i2} &= (\Delta z_{i2}\Delta\gamma_{11}-\Delta z_{i1}\Delta\gamma_{12})B^{-1}, \end{aligned}\right\} \qquad (3.15)$$

where

$$\Delta z_{iJ} = (z_{iJ}-\bar{z}_i), \quad B = \Delta\gamma_{11}\Delta\gamma_{22}-\Delta\gamma_{12}\Delta\gamma_{21}. \qquad (3.16)$$

In (3.15) and (3.16), Z and z stand for either X and x or Y and p. The symbols x_{iJ} and p_{iJ} denote the i-th coordinate and i-th component of the slowness vector on the J-th auxiliary ray for the time τ, see (3.13). The symbols $\bar{x}_i$ and $\bar{p}_i$ denote the corresponding quantities on the central ray. The symbol $\Delta\gamma_{IJ}$ denotes the difference between the I-th ray parameter of the J-th auxiliary ray and the central ray. Formulae (3.15) and (3.16) are applicable to both isotropic and anisotropic media.

The matrix X_{ij} is very closely related to the function J, see (2.15). It follows immediately from (2.15) that

$$J = V^{-1}\det(X_{ij}). \qquad (3.17)$$

A change of the sign of the determinant $\det(X_{ij})$ indicates that the considered ray touched a caustic.

3.6 CONSTRUCTION OF RAY SYNTHETIC SEISMOGRAMS

To construct ray synthetic seismogram at a given receiver, the following quantities must be known at the receiver for each elementary wave: the travel time from the source to receiver and the complex vector amplitude including geometrical spreading. The evaluation of these quantities at the receiver practically always involves the application of the paraxial ray approximation.

The paraxial ray approximation may be applied in many ways. The simplest way is the use of the paraxial ray approximation from the end-point of the ray which is closest to the desired receiver. Other possibilities are to use various weighted summations of paraxial ray approximations from several points which are closest to the receiver. The latter approach is close to the method of summation of Gaussian beams.

In the first programs based on the described algorithm we adopted the first approach. A search is made for all endpoints of rays falling within a given radius of each receiver. If such endpoints exist, the endpoint closest to the receiver is used for the application of the paraxial ray approximation. If there is no endpoint in the vicinity, the receiver is considered to be situated in a shadow region of the investigated elementary wave.

As soon as the travel time and vectorial amplitude are known at the receiver, an elementary synthetic seismogram and then a ray synthetic seismogram are constructed. A modified program SYNTPL from the ray package SEIS83 (Červený and Pšenčík 1984) is used for this purpose.

4 Numerical examples

Two program packages based on the algorithm described in the previous section have been written:

The package called ANRAY86 (Gajewski and Pšenčík 1986) is designed for the computation of travel times and spreading-free vectorial amplitudes along rays terminating on straight profiles situated on the model surface and passing through the epicentre. The boundary-value ray tracing used to find such rays is based on the shooting method. A modified shooting procedure from the ray package SEIS83 (Červený and Pšenčík 1984) is used for this purpose.

The package called SEISAN86 is designed for the computation of ray synthetic seismograms using the procedure of the paraxial ray approximation described in the previous sections. The contributions of individual elementary waves to a given receiver are evaluated from the values determined along a ray with its endpoint closest to the receiver. To guarantee a sufficient density of endpoints of rays in the vicinity of receivers, the modified shooting procedure from the ray package SEIS83 is used again. In this case the procedure determines the rays that terminate in the prescribed vicinity of concentric circles around the source with radii equal to the epicentral distances of individual receivers. At present, the density of endpoints of rays of individual elementary waves is checked visually; in places with insufficient density of endpoints, additional rays are shot.

The program package SEISAN86 has been applied to the study of wave propagation in the ANVIL model of an anisotropic subcrustal lithosphere, which was proposed by Fuchs (1983) to explain the P-wave travel time and amplitude variations in south Germany. Here we use the ANVIL model only as a test model in order to present examples of results computed with SEISAN86, and no conclusions concerning the lithospheric structure in south Germany are made here. A more detailed investigation of the model with package SEISAN86, including some preliminary conclusions, can be found in Gajewski and Pšenčík (1987).

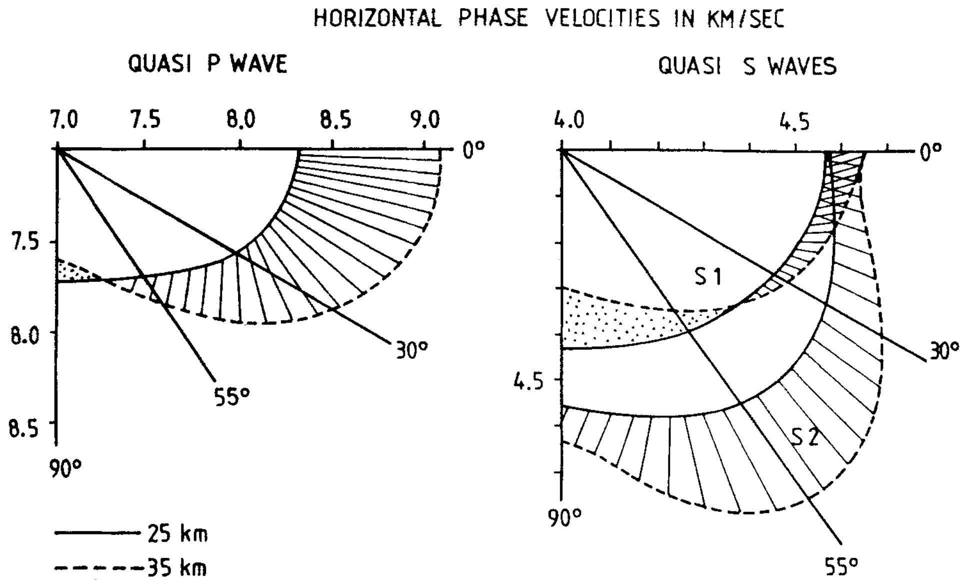

Figure 1. Anisotropic (orthorhombic) layer of the ANVIL model - a model of the continental, subcrustal anisotropic lithosphere suggested by Fuchs (1983). Horizontal phase velocities of *qP*-waves (on left) and *qS*-waves (on right) at 25 km depth (solid lines) and 35 km depth (broken lines). Hatched areas, and dotted areas, denote the regions of positive, and negative, vertical gradient of horizontal phase velocity, respectively. The crust is homogeneous, V_P = 6.5 km/sec, V_S = 3.75 km/sec, and 25 km thick. Profiles along 0^o, 30^o, 55^o, and 90^o directions are indicated.

The part of the ANVIL model used for the computations has the following structure. The crust is isotropic, 25 km thick, with constant *P*- and *S*-wave velocities (6.5 and 3.75 km/sec). The upper mantle consists of an anisotropic orthorhombic layer underlain by an isotropic halfspace with constant *P*- and *S*-wave velocities (8.1 and 4.67 km/sec). The anisotropic layer is 10 km thick. The elastic parameters specified at the top and the bottom of the layer vary linearly through the layer. The elasticity tensor rotates linearly between the interfaces bounding the layer, making the total rotation of 3.6^o. Figure 1 shows the azimuthal dependence of horizontal *qP* and *qS* phase velocities at depths of 25 km (solid line), and 35 km (dashed line), corresponding to the top, and bottom of the anisotropic layer. More details on the whole ANVIL model can be found in Fuchs (1983) and Gajewski and Pšenčík (1987).

In Figures 2 and 3, ray synthetic seismograms along profiles 0^o and 55^o (see Fig. 1) are shown. All possible refracted and primary reflected waves including those with conversion at the point of reflection are considered. In addition, the twice reflected and refracted *qP*-waves in the anisotropic layer are considered.

The source is situated immediately below the surface of the isotropic

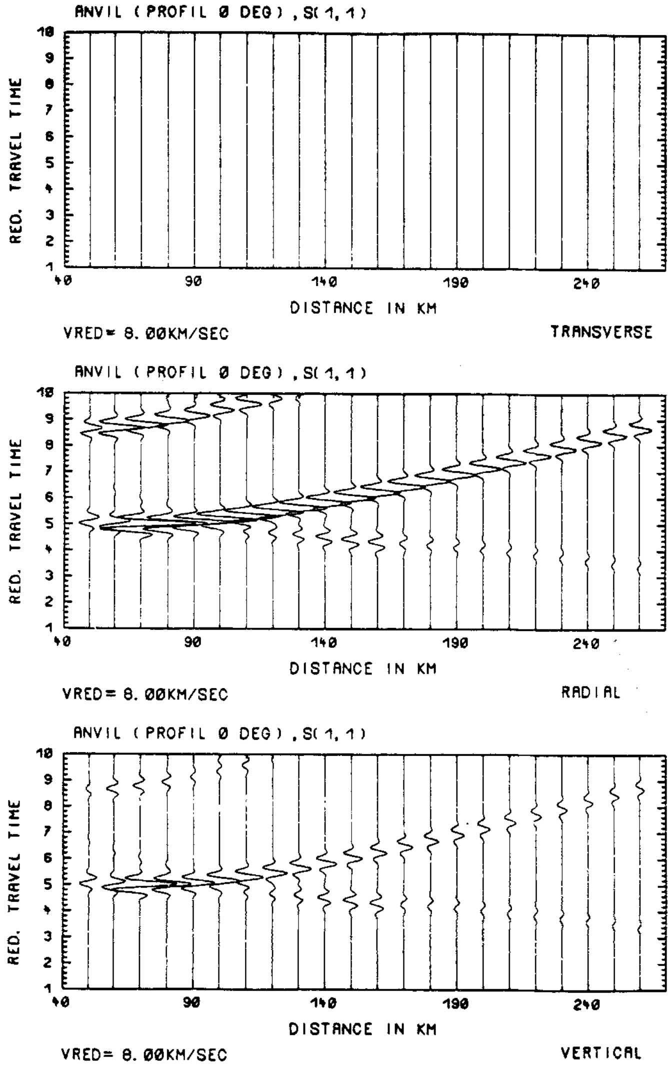

Figure 2. Ray synthetic seismograms of transverse, radial and vertical components of the displacement vector for the profile along 0^o direction in the ANVIL model of Fig.1, showing predominantly P-wave arrivals. The strongest arrival is the P-wave reflection from the crust-mantle boundary. The principal frequency of the source signal is 2 Hz.

crust, at the origin of coordinates. It is the artificial point source described in Section 3.2, radiating both P- and S-waves. The amplitudes on the unit sphere around the source are equal to 1.0 for the P-waves, and to 1.41 for the *S*-waves. The polarization vectors of the *S*-waves are chosen for each ray in such a way that the *S*-wave has equal *SV* and *SH* components at the source. As a source-time function, the Gaussian envelope signal (3.6) with the prevailing frequency of 2 Hz is used. A time shift of 0.48 sec is used to shift the signal so that the arrival

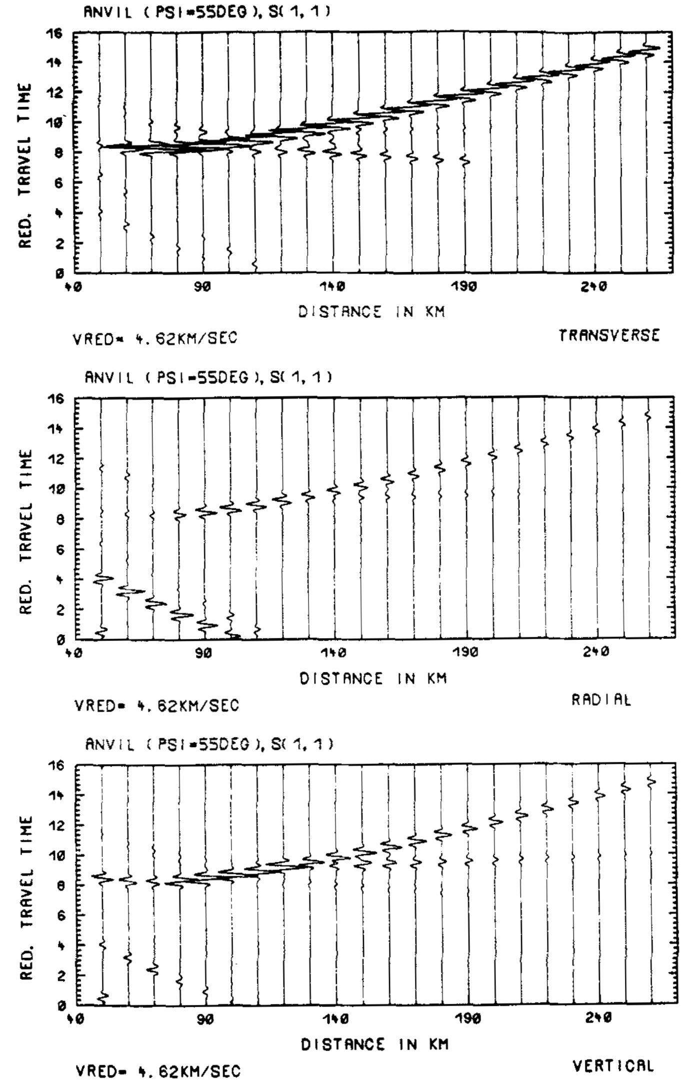

Figure 3. Ray synthetic seismograms of transverse, radial and vertical components of the displacement vector for the profile along 55° direction in the ANVIL model of Fig.1, showing predominantly *S*-wave arrivals. The strongest arrival is the reflection from the crust-mantle boundary. Preceding arrivals are due to shear wave splitting in the subcrustal anisotropic layer. The principal frequency of the source signal is 2 Hz.

time corresponds to the onset of the signal. No amplitude-power scaling is used, neither along the profiles nor along individual traces.

The seismograms in Fig. 2 are recorded along a profile in the direction 0° (Fig.1). Due to the chosen reduction velocity and the time window, the figure mostly shows *P* arrivals. Since the direction of the profile corresponds to the direction with small anisotropic effects (nearly symmetry plane, see Fig. 1), the *P*-waves have non-observable transverse components.

The dominant wave on the radial and vertical components is the reflection from the crust-mantle interface. The preceding wave is an interference of P-waves once and twice reflected and refracted in the anisotropic layer. These reflections are all subcritical since along the 0^o profile the phase velocities in the anisotropic layer are greater than those in the underlying halfspace.

The seismograms in Fig. 3 are recorded along profile 55^o, see Fig. 1. In this case the reduction velocity and the time window are chosen in such a way as to show mostly *S*-wave arrivals. The anisotropic effects are strongest along this profile. The most prominent wave is again the reflection from the crust-mantle interface which can be now observed on all three components. This wave is preceded by two branches, both of which are seen between 150 and 190 km. This is an exhibition of the shear -wave splitting phenomenon. The two branches are caused by two *qS*-waves propagating in the anisotropic layer. The faster one is caused by the interference of refracted and reflected phases of one of the *qS*-waves in the anisotropic layer. The slower one is caused by the reflection of the other *qS*-wave. The refracted phase of the slower *qS*-wave does not exist since this wave has a negative gradient in the anisotropic layer for this direction.

5 Conclusions

An algorithm for the computation of ray synthetic seismograms in 3-D laterally inhomogeneous structures consisting of a combination of isotropic and anisotropic layers has been proposed. Program packages have been written, based on this algorithm, which make possible the computation of travel times, vectorial amplitudes and ray synthetic seismograms on the surface of complex 3-D models.

The programs can be applied to the investigation of various theoretical aspects of seismic wave propagation in anisotropic media. This may include the study of problems of shear-wave splitting, reflection/transmission, polarization of shear waves and other phenomena, which may serve as indications of anisotropy, or may be used to separate the effects of anisotropy from the effects of inhomogeneity. The algorithm and the present programs can be also used to the solution of problems of practical interest. An example is the application of package SEISAN86 to the ANVIL model of the continental subcrustal lithosphere, as in the numerical examples in the previous section and the more detailed study in Gajewski and Pšenčík (1987). Last but not least, the programs can also be used effectively in the study of 3-D isotropic problems. The procedures for isotropic layers are independent and only use the formulae for isotropic media.

The algorithm and corresponding programs still need some testing and refinement. The model should be generalized to allow modelling of block structures, vanishing layers, isolated bodies, etc. The approximate procedure for the determination of the geometrical spreading should be tested for effectiveness and accuracy against a procedure based on dynamic ray tracing. The procedure for the generation of the end-points of rays in an investigated region also needs refinement. It would be desirable also to investigate the limits of applicability of the algorithm and programs in special situations such as singular regions, and regions in which the phase velocities of *qS*-waves are close to each other. Such investigation should include comparison with the results of more exact methods where these are applicable.

Possible modifications and generalizations:

(1) The described packages can be easily modified for applications in seismic prospecting - computations of normal incidence synthetic sections, vertical seismic profiling, cross-hole shooting, or in microzoning - seismic response computations. The programs could also be modified for studies of the combined effects of source and anisotropy of the medium in focal zones. More general types of sources, including more general source-time functions, could also be introduced.

(2) The present use of "single" paraxial ray approximation in the evaluation of synthetic seismograms could be substituted by a procedure based on the weighted summation of paraxial ray approximations, or possibly by Gaussian beam summation.

(3) Specialized programs could be derived from the present packages, which could more effectively deal with some simpler types of seismic anisotropy.

Acknowledgements

The authors wish to thank Prof. K. Fuchs for encouraging this study and fruitful discussions, and to Prof. V. Červený and Prof. A. Hanyga for critically reading the manuscript of the paper. The cooperation of Luděk Klimeš, who provided comparative computations with his 3-D 'isotropic' program package, and valuable comments, is greatly appreciated.

References

Aki, K. & Richards, P., 1980. Quantitative Seismology, W.H. Freeman, San Francisco.

Babich, V.M., 1961. Ray method for the computation of the intensity of wave fronts in elastic inhomogeneous anisotropic medium, in: *Problems of the Dynamic Theory of Propagation of Seismic Waves*, **5**, 36-46, Leningrad University Press, Leningrad (in Russian).

Červený, V., 1972. Seismic rays and ray intensities in inhomogeneous anisotropic media, *Geophys.J.R.astr.Soc.*, **29**, 1-13.

Červený, V., 1985. The application of ray tracing to the numerical modelling of seismic wavefields in complex structures, in: *Handbook of Geophysical Exploration, Section 1: Seismic Exploration*, eds Helbig, K. & Treitel, S., *Seismic Shear Waves*, 1-124, ed. Dohr. G., Geophysical Press, London.

Červený, V. & Firbas, P., 1984. Numerical modelling and inversion of travel times of seismic body waves in inhomogeneous anisotropic media, *Geophys.J.R.astr.Soc.*, **76**, 41-51.

Červený, V., Klimeš, L. & Pšenčík, I., 1984. Paraxial ray approximations in the computation of seismic wavefields in inhomogeneous media, *Geophys.J.R.astr.Soc.*, **79**, 89-104.

Červený, V., Klimes, L. & Pšenčík, I., 1986. Complete seismic ray tracing in 3-D layered structures, in: *Seismological Algorithms*, ed. Doornbos, D.J., Academic Press, submitted.

Červený, V., Molotkov, I.A. & Pšenčík, I., 1977. *Ray Method in Seismology* Charles University Press, Prague.

Červený, V. & Pšenčík, I., 1984. SEIS83 - Numerical modelling of seismic wave fields in 2-D laterally varying layered structures by the ray method, in: *Documentation of Earthquake Algorithms, Report SE-35*, ed. Engdahl, E.R., World Data Centre (A) for Solid Earth Geophysics, Boulder.

Crampin, S., 1981. A review of wave motion in anisotropic and cracked elastic-media, *Wave Motion*, **3**, 343-391.

Daley, P.F. & Hron, F., 1977. Reflection and transmission coefficients for transversely isotropic media, *Bull.seism.Soc.Am.*, **67**, 661-675.

Dellinger, J. & Muir, F., 1986. Axisymmetric Anisotropy I: Kinematics, in: *Stanford Exploration Project* (J.F. Claerbout, ed.), Rep. No. 42, Department of Geophysics, Stanford University.

Fedorov, F.I., 1968. *Theory of Elastic Waves in Crystals*, Plenum Press, New York.

Fuchs, K., 1983. Recently formed elastic anisotropy and petrological models for the continental subcrustal lithosphere in Southern Germany, *Phys.Earth.Plant.Inter.*, **31**, 93-118.

Gajewski, D. & Pšenčík, I., 1986. *Numerical modelling of seismic wave fields in 3-D laterally varying layered anisotropic structures - Program ANRAY86*, Internal Report Inst.of Earth and Planet.Phys., University of Alberta, Edmonton.

Gajewski, D. & Pšenčík, I., 1987. Ray synthetic seismograms for a 3-D anisotropic lithospheric structure, *Phys.Earth Planet.Int.*, in press.

Hanyga, A., 1984. Point source in anisotropic elastic medium, *Geophysik*, **93**, 463-479.

Hanyga, A., 1986a. *Numerical methods of tracing rays and wavefronts, Seismological Algorithms*, ed. Doornbos, D.J., Academic Press, submitted.

Hanyga, A., 1986b. Gaussian beams in anisotropic media, *Geophys.J.R.astr.Soc.*, **85**, 473-503.

Henneke, E.G., 1972. Reflection-refraction of a stress wave at a plane boundary between anisotropic media, *J.acoust.Soc.Am.*, **51**, 210-216.

Kravtsov, Yu.A. & Orlov, Yu.I., 1980. *Geometrical Optics of Inhomogeneous Media*, Nauka, Moscow (in Russian).

McMechan, G.A. & Mooney, W.D., 1980. Asymptotic ray theory and synthetic seismograms for laterally varying structure: Theory and application to the Imperial Valley, California, *Bull.seism.Soc.Am.*, **70**, 2021-2035.

Musgrave, M.P.J., 1970. *Crystal Acoustics*, Holden-Day, San Francisco.

Petrashen, G.I. & Kashtan, B.M., 1984. Theory of body wave propagation in inhomogeneous anisotropic media, *Geophys.J.R.astr.Soc.*, **76**, 29-39.

Šílený, J., 1981. Anomalous behaviour of seismic waves at an interface between anisotropic media, *Studia geoph.et.geod.*, **25**, 152-159.